

Title	The Crystallization Kinetics of Glassy Fe ₄₀ Ni ₄₀ P ₂₀
Author(s)	Naka, Masaaki; Okamoto, Ikuo
Citation	Transactions of JWRI. 1981, 10(2), p. 213-218
Version Type	VoR
URL	https://doi.org/10.18910/8391
rights	
Note	

Osaka University Knowledge Archive : OUKA

<https://ir.library.osaka-u.ac.jp/>

Osaka University

The Crystallization Kinetics of Glassy $\text{Fe}_{40}\text{Ni}_{40}\text{P}_{20}$ [†]

Masaaki NAKA* and Ikuo OKAMOTO**

Abstract

The crystallization kinetics of glassy $\text{Fe}_{40}\text{Ni}_{40}\text{P}_{20}$ have been determined by transmission electron microscopy and electrical resistivity measurements. The glassy alloy crystallizes isochronally by two stages at heating rate of 5 K/min. First, amorphous phase transforms to (Fe, Ni) austenite and (Fe, Ni)₃P phases by a eutectic reaction at 623 K. Second, the eutectic phases recrystallize into the stable phase structure of the same phases at 873 K.

The data of isothermal anneals of the first process at the temperatures between 603 and 633 K are interpreted by use of the Johnson-Mehl-Avrami equation for the transformation theory. The time dependence in J-M-A equation is constant $t^{1.5}$ between 603 and 618 K, but increases to $t^{3.2}$ at 633 K. The activation energy for the first process is observed to be 85 kcal/mol, which is lower than that of $\text{Fe}_{40}\text{Ni}_{40}\text{P}_{14}\text{B}_6$ glass.

KEY WORDS: (Metallic Glasses) (Crystallization Kinetics) (Iron Glass) (Isothermal Annealing)

1. Introduction

The crystallization behavior of iron-base glasses containing about 20 at.% metalloid content has recently attracted considerable attention. Alloys such as $\text{Fe}_{40}\text{Ni}_{40}\text{P}_{14}\text{B}_6$ (1)-4) and $\text{Fe}_{80}\text{B}_{20}$ (5)-7) are some of the more extensively studied in this area. Herold and Köster⁷⁾ have shown that the crystallization of $\text{Fe}_{100-x}\text{B}_x$ glasses is interpreted in terms of a diagram of the free energy for crystalline phase versus constituent concentration, and glassy alloys decompose into crystalline phases by three types: polymorphous, primary and eutectic crystallization. Therefore, the overlap of two or more crystallization processes often prevents the interpretation of crystallization kinetics of metallic glasses. On the other hand, Watanabe and Scott⁴⁾ have reported that $\text{Fe}_{40}\text{Ni}_{40}\text{P}_{14}\text{B}_6$ alloy crystallizes by a eutectic mechanism to form Fe-Ni austenite and a (Fe, Ni)₃(P, B) body-centred tetragonal phase, and the crystallization kinetics can be analysed by the Johnson-Mehl equation with an exponent of 4.

This paper reports crystallization kinetics of eutectic reaction of $\text{Fe}_{40}\text{Ni}_{40}\text{P}_{20}$ alloy.

2. Experimental Procedures

The metallic glass samples were prepared as ribbons, about 2 mm wide and 20 μm thick, by rapid quenching from the melt using a melt spinning technique. Electrical resistivity was measured with an ordinary four terminal

method. The isochronal and isothermal annealing were carried out in evacuated quartz tube or silicon oil bath, respectively. The structure of heat-treated specimens were examined by X-ray diffraction with $\text{Fe}\cdot\text{K}\alpha$ radiation. The thin parts of splat-quenched sample were used for the transmission electron microscopy in a hot stage at heating rate of about 5 K/min.

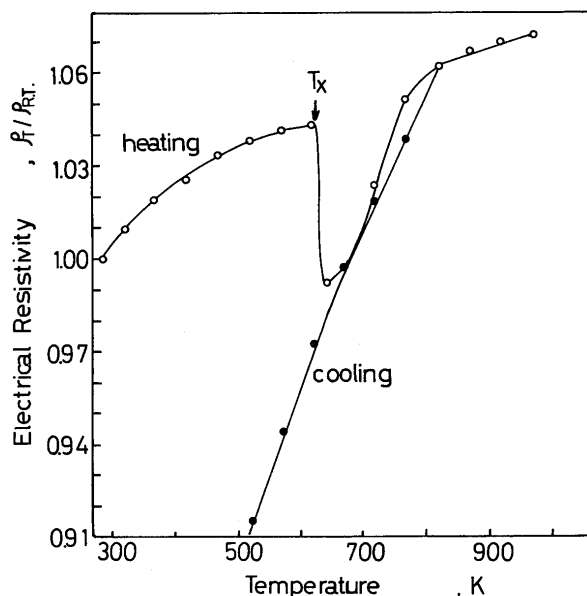


Fig. 1 Change in electrical resistivity ρ_T / ρ_{RT} of $\text{Fe}_{40}\text{Ni}_{40}\text{P}_{20}$ alloy during isochronal anneals.

[†] Received on October 9, 1981

* Associate Professor

** Professor

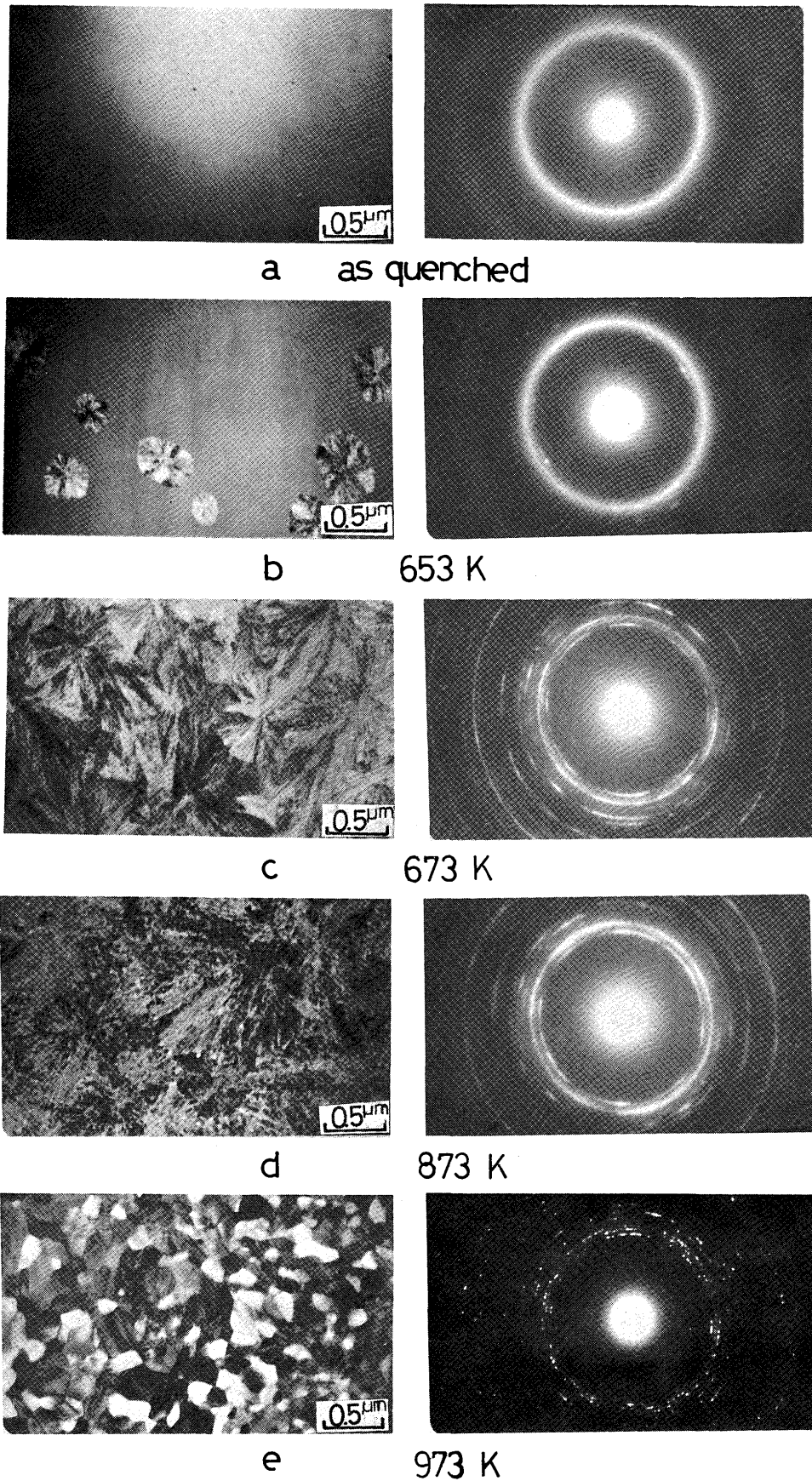


Fig. 2 Transmission electron micrograph and diffraction pattern of sample heated under dynamic condition.

(a) as received, (b) 653 K, (c) 673 K, (d) 973 K at heating rate of 5 K/min.

3. Results and Discussion

Figure 1 shows the electrical resistivity of $\text{Fe}_{40}\text{Ni}_{40}\text{P}_{20}$ as a function of temperature with a heating or cooling rate of about 5 K/min. The alloy shows a relatively small but positive temperature coefficient of the resistivity in the amorphous region, followed by a sharp decrease as the crystallization process started. The one set of this decrease has been taken as the crystallization temperature T_x ($= 623$ K).

The change in microstructure of $\text{Fe}_{40}\text{Ni}_{40}\text{P}_{20}$ alloy with temperature were observed at a heating rate of about 5 K/min in the hot stage of transmission microscope as shown in Fig. 2. The alloy shows two crystallization processes at the isochronal annealing up to 1000 K. In the first process the specimens contain a uniform distribution of spherulitic crystals at 635 and 673 K as shown in Fig. 2 (b, c). In order to identify the crystalline phase X-ray diffraction patterns of specimen annealed for 90 min at 613 K were obtained by Debye-Scherrer method in Table 1. Most of the X-ray reflections can be indexed on a bct phase having $(\text{Fe, Ni})_3\text{P}$ structure ($a = 9.02$, $c = 4.44$ Å). A careful comparison of the observed intensity with values of $(\text{Fe, Ni})_3\text{P}$ is ASTM card⁸⁾ indicates there is also a fcc phase ($a = 3.51$ Å). Therefore, $\text{Fe}_{40}\text{Ni}_{40}\text{P}_{20}$ alloy transformed to (Fe, Ni) austenite and a $(\text{Fe, Ni})_3\text{P}$ phase with a lamellar structure, which is

analogous to the crystalline structure of $\text{Fe}_{40}\text{Ni}_{40}\text{P}_{16}\text{B}_6$ alloy⁴⁾.

In the second process at 873 and 973 K in Fig. 2 (d, e) the lamellar structure changes to stable structure. From X-ray diffraction analysis the crystalline phase in the stage are also austenite and $(\text{Fe, Ni})_3\text{P}$ phase, and the second crystallization process is the recrystallization of the grain growth of lamellar structure of (Fe, Ni) austenite and $(\text{Fe, Ni})_3\text{P}$ phases.

The data for the first annealing process will be interpreted in terms of the generalized transformation theory⁹⁾.

$$X = \frac{R_0 - R_t}{R_0 - R_\infty} = 1 - \exp(-kt)^n \quad (1)$$

Where X is the volume fraction transformed, k a kinetic constant, t the time and $t = 0$ is taken as the end of the incubation period, R_0 , R_t , R_∞ , electrical resistance at time 0, t and ∞ , respectively. The transformation fraction X at the temperatures between 603 and 633 K is given in Fig. 3. The parameters n and k in eq. (1) are estimated by plotting $\ln \ln(1/1-X)$ versus $\ln t$. As shown in Fig. 4 the linear relations exist between them for $X = 0.05 \sim 0.08$.

The J-M-A exponent n in Fig. 5 was within experimental uncertainty constant at about 1.5 between 603

Table 1 X-ray diffraction analysis of specimen annealed for 70 min at 613 K.

number	$d_{\text{obs.}}$ (Å)	Intensity	$(\text{Fe, Ni})_3\text{P}$ in ASTM card			(Fe, Ni) austenite
			d (Å)	(hkl)	I/I_1	(hkl)
1	2.494	W.	2.50	(301)	25	
2	2.180	V. S.	2.19	(321)	100	
3	2.100	V. S.	2.11	(112)	70	
4	2.009	V. S.	2.02	(420)	50	(111)
5	1.970	V. S.	1.972	(411)	70	
6	1.822	M.	1.833	(222)	35	
7	1.749	S.	1.778	(510)	25	(200)
8	1.270	S.	1.274	(710)	30	(220)
9	1.223	V. W.	1.234	(413)	14	
10	1.197	V. W.	1.205	(622)	14	
11	1.106	W.	1.097	(820)	25	
12	1.088	W.	1.075	(660)	18	

V.S. : very strong intensity of X-ray diffraction, S. : strong intensity, W. : weak intensity, V. W. : very weak intensity.

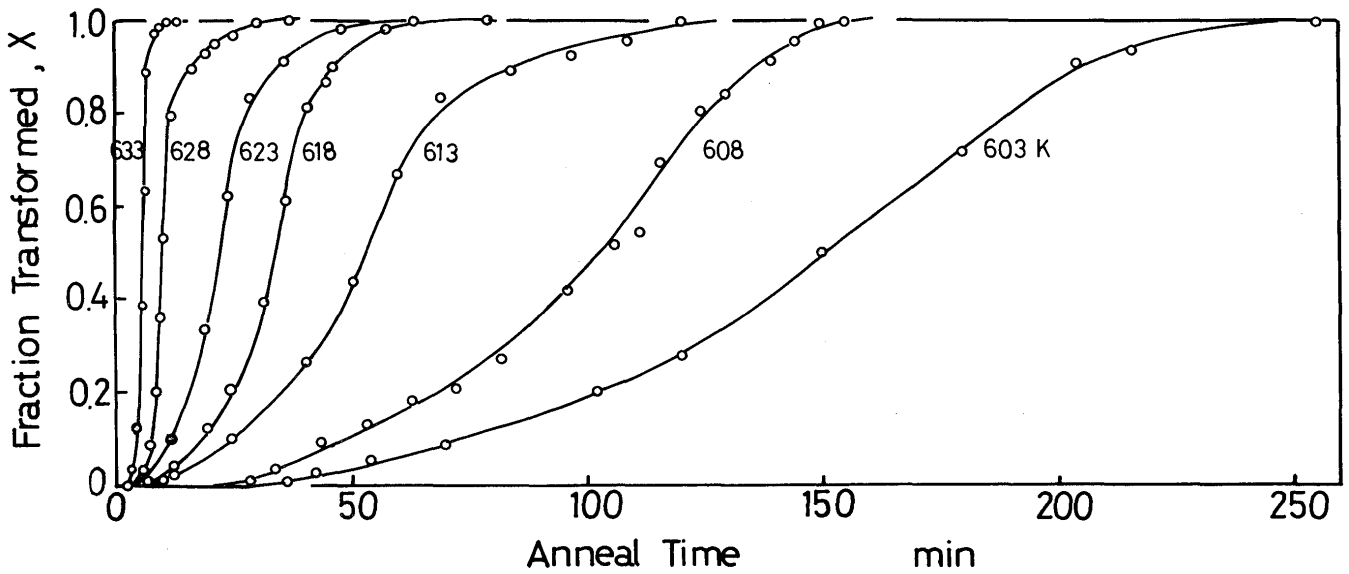


Fig. 3 Fraction, X, transformed versus the time in minutes during isothermal anneal between 603 and 633 K.

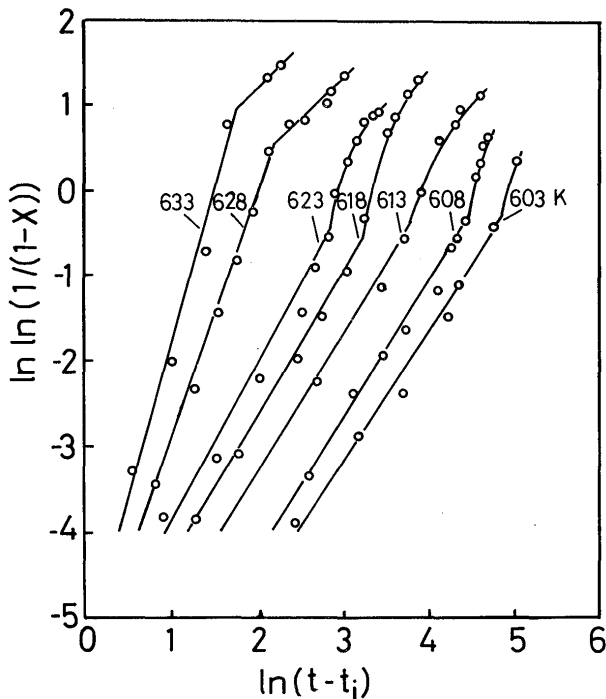


Fig. 4 Fit of X for specimens isothermally annealed to Johnson-Mehl-Avrami equation. t_i is the crystallization start time.

and 618 K, but increased linearly to 3.2 between 623 and 633 K. According to the theory of phase transformation⁹⁾, the crystallization process of $\text{Fe}_{40}\text{Ni}_{40}\text{P}_{20}$ alloy changes from a diffusion controlled growth with constant nucleation sites ($n = 1.5$) at lower temperatures to a interface diffusion controlled growth with constant nucleation sites ($n = 3$) at higher temperatures. The value ($n = 4$) of $\text{Fe}_{40}\text{Ni}_{40}\text{P}_{16}\text{B}_6$ alloy reported by Watanabe

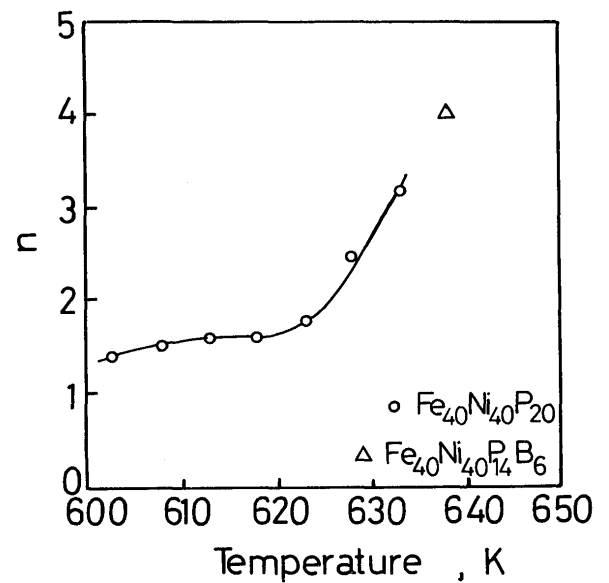


Fig. 5 Variation of the Johnson-Mehl-Avrami exponent (n) of $\text{Fe}_{40}\text{Ni}_{40}\text{P}_{20}$ alloy with isothermal annealing temperature, and n of $\text{Fe}_{40}\text{Ni}_{40}\text{P}_{14}\text{B}_6$ alloy⁴⁾ is also included.

and Scott⁴⁾ is also included in Fig. 5.

The activation energy E for the crystallization process can be obtained from the temperature dependence of k and Arrhenius relation⁹⁾.

$$k = k_0 \exp(-E/k_B T) \quad (2)$$

where k is a constant and k_B is Boltzmann constant. From the results shown in Fig. 6, the activation energy for the crystallization was (85 ± 1) kcal/mol. Watanabe and Scott⁴⁾ have indicated that $\text{Fe}_{40}\text{Ni}_{40}\text{P}_{14}\text{B}_6$ alloy also

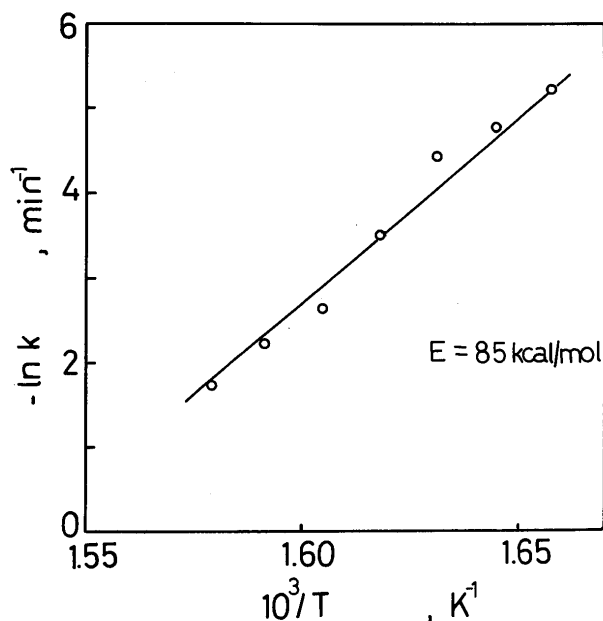


Fig. 6 The \ln of the kinetic constant k against reciprocal temperature in $\text{Fe}_{40}\text{Ni}_{40}\text{P}_{20}$.

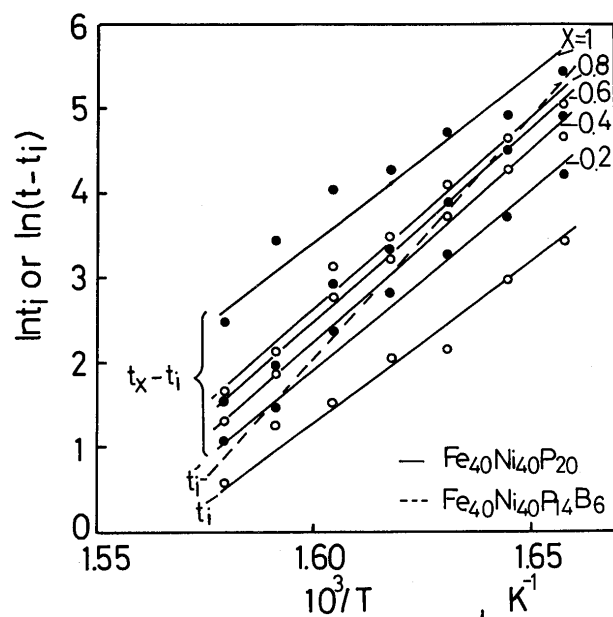


Fig. 7 Temperature dependence of time for fraction for the crystallization, where t is the anneal time and t_i is the crystallization start time. t_i of $\text{Fe}_{40}\text{Ni}_{40}\text{P}_{14}\text{B}_6$ is also included for the comparison.

decomposes into fcc phase and $(\text{Fe}, \text{Ni})_3(\text{P}, \text{B})$ phase by a eutectic reaction which possesses 102 kcal/mol of the activation energy for the crystallization. The replacement of P with B increases the activation energy of crystallization and stabilizes $\text{Fe}_{40}\text{Ni}_{40}\text{P}_{20}$ alloy.

Activation energy for the crystallization may be alternatively obtained from the time t_x to a fraction crystallized X at a temperature⁹⁾.

$$t_x \propto k^{-1} \exp(E/k_B T) \quad (3)$$

In this way an activation energy can be obtained from the slope E/k_B of plots of $\ln t_i$ or $\ln(t-t_i)$ against $1/T$ as shown in Fig. 7, where t_i is the crystallization start time. The activation energies from the beginning to the end of the crystallization are approximately constant (85 ± 3) kcal/mol, and agree well with the values obtained in equation (2). t_i of $\text{Fe}_{40}\text{Ni}_{40}\text{P}_{14}\text{B}_6$ alloy is also included in the figure.

Second, the energy for the crystallization can be determined from the rapid change in temperature from T_1 to T_2 during annealing at T_1 . On the assumption⁹⁾ that a fraction crystallized X is constant at both T_1 and T_2 at the rapid change of the temperature.

$$\ln\left(\frac{dX}{dt}\right)_{T_2} - \ln\left(\frac{dX}{dt}\right)_{T_1} = \frac{E}{k_B} \left(\frac{1}{T_1} - \frac{1}{T_2}\right) \quad (4)$$

As shown in Fig. 8 the annealing temperature changed abruptly from 603 to 613 K. The activation energies obtained from two fractions of X are 62 and 70 kcal/mol

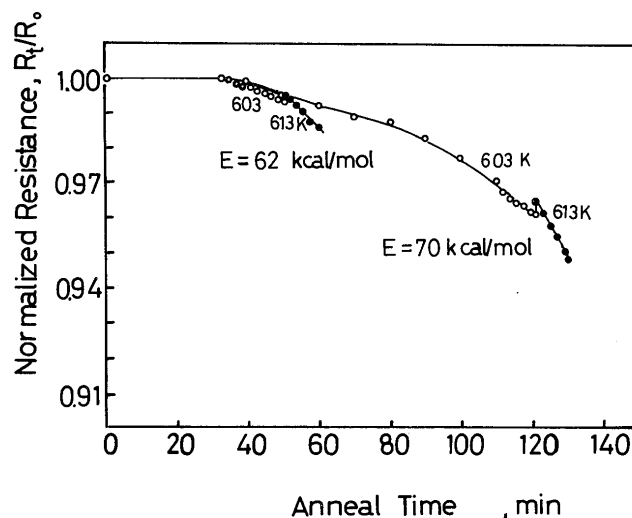


Fig. 8 Abrupt change of anneal temperature from 603 to 613 K during annealing at 603 K.

which are lower than obtained from equation (2). This difference may arise from that the nucleation sites of crystalline phases change by the abrupt heating.

4. Conclusions

The isothermal crystallization kinetics of $\text{Fe}_{40}\text{Ni}_{40}\text{P}_{20}$ glass has been investigated at temperatures between 603 and 633 K. $\text{Fe}_{40}\text{Ni}_{40}\text{P}_{20}$ glass transforms to (Fe, Ni)

austenite and $(\text{Fe, Ni})_3\text{P}$ phase by a eutectic mechanism. The kinetics are found to obey the Johnson-Mehl-Avrami relationship, $X = 1 - \exp(-kt)^n$, where X is the volume fraction crystallized, n is a coefficient and k is a kinetic constant that obeys the Arrhenius relationship. n is about 1.5 between 603 and 618 K, but increases to 3.2 at 633 K. The activation energy for the crystallization is 85 kcal/mol.

Acknowledgement

The authors acknowledge helpful discussions with Professor T. Masumoto and Dr. A. Inoue of The Research Institute for Iron, Steel and Other Metals of Tohoku University.

References

- 1) J.L. Walter, P. Rao, E.F. Koch and S.F. Bartram: *Met. Trans.*, 8A (1977), 1141.
- 2) M.G. Scott: *J. Mater. Sci.*, 13 (1978), 291.
- 3) M.G. Scott: *Proc. 3rd Inter. Conf. Rapidly Quenched Metals*, ed., by B. Cantor, (The Metals Society, London, 1978), Vol. 1, P. 198.
- 4) T. Watanabe and M. Scott: *J. Mater. Sci.*, 15 (1980), 1131.
- 5) J.L. Walter and S.F. Bartram: *Proc. 3rd Inter. Conf. Rapidly Quenched Metals*, ed., by B. Cantor, (The Metals Society, London, 1978), Vol. 1, P. 307.
- 6) T. Kemeny, I. Vinze, B. Fograssy and S. Arajs: *Proc. 3rd Inter. Conf. Rapidly Quenched Metals*, ed., by B. Cantor, (The Metals Society, London, 1978), Vol. 1, P. 291.
- 7) U. Herold and U. Köster: *Proc. 3rd Inter. Conf. Rapidly Quenched Metals*, ed., by B. Cantor, (The Metals Society, London, 1978), Vol. 1, p. 281.
- 8) H. Chao, I. Dwornicke and W. Littler: *Geochim. Cosmochim. Acta* 28 (1964), 971, X-ray data card of ASTM no. 16-707.
- 9) J. Burke: "The Kinetics of Phase Transformations in Metals", (Pergamon Press, England, 1965).